

RADIOCHEMISTRY AND RADIOPHARMACEUTICALS

C-11 Dimethyloxazolidinedione (DMO): Biodistribution, Radiation Absorbed Dose, and Potential for PET Measurement of Regional Brain pH:
Concise Communication

Kimberlee J. Kearfott, Larry Junck, and David A. Rottenberg

Memorial Sloan-Kettering Cancer Center, New York, New York

An improved radiochemical synthesis for C-11 dimethyloxazolidinedione (C-11 DMO) makes this agent attractive for the measurement of regional brain tissue pH (rpH) using positron emission tomography (PET). Toward this end, biodistribution data for C-14 DMO in rats at various times after an intravenous bolus injection are reported, together with estimates of radiation absorbed dose for C-11 DMO in man. An error analysis of C-11 DMO PET measurement of rpH indicates that rpH can be determined to within ± 0.1 pH unit for pH > 6.5 with a 20-mCi injected bolus of C-11 DMO, a 30-45-min equilibration time, and a 15-min PET imaging period.

J Nucl Med 24: 805-811, 1983

The study of regional cerebral acid-base status in vivo using positron emission tomography (PET) and $^{11}\text{CO}_2$ has been proposed (1). However, the validity of the CO_2 approach to the measurement of brain pH has been called into question by Lockwood et al. (2), who concluded that CO_2 fixation by brain is substantial. The equilibrium distribution of dimethyloxazolidinedione (DMO) may be used to estimate tissue pH (3-5), and DMO has been labeled with C-11 for use with PET by Ginos et al. (6).

This paper presents data pertinent to the use of C-11 DMO in human subjects, namely: (a) the biodistribution of C-14 DMO in the rat, (b) estimates of radiation absorbed dose for C-11 DMO in man based on the C-14 DMO rat biodistribution data, and (c) an error analysis of C-11 DMO PET measurements of regional brain-tissue pH (rpH).

METHODS

Biodistribution and in vivo kinetics. The biodistribution of DMO was studied by injecting 15-25 μCi C-14-la-

beled DMO intravenously into Wistar rats (210-450 g), which were killed by decapitation at 5, 15, 30, 60, or 120 min (3-4 animals per time point). Animals were preloaded with 10 mg/kg of nonradioactive DMO before the administration of C-14-labeled DMO to saturate "reverse" choroid plexus transport of DMO from cerebrospinal fluid (7). This preloading results in a maximum estimated acid load of 0.09 $\mu\text{mole/g}$ brain (neglecting excretion before and during the study). Duplicate samples obtained from various tissues and from the gastrointestinal contents were blotted and weighed, digested with solubilizer, and decolorized to form 15-ml cocktails, which were then counted in a liquid scintillation spectrometer. Quench corrections were made by external standardization using known amounts of C-14 hexadecane or C-14 toluene at various quench levels. To investigate the dependence of urinary pH on DMO excretion, bladder catheters were placed in four animals, and urine was sampled serially for C-14 DMO concentration and pH while NaHCO_3 , ascorbic acid, or dilute HCl was administered intravenously to alter urine pH.

Calculations of radiation absorbed dose. The individual organ concentration per whole-body concentration was assumed to be the same for rats and humans. Hence, the percent injected dose per organ (i) in humans (%ID/O)

Received May 18, 1982; revision accepted Apr. 6, 1983.

For reprints contact: K. J. Kearfott, ScD, Dept. of Neurology, Memorial Sloan-Kettering Cancer Center, 1275 York Ave., New York, NY 10021.

was estimated from the tissue-plasma partition coefficient for C-14 DMO in rats (p , tissue-to-plasma concentration ratio) using:

$$(\%ID/O)_{human} = (p_i)_{rat} \times \left(\frac{A_b/m_b}{A_{TB}/m_{TB}} \right)_{rat} \times \left(\frac{m_i}{m_{TB}} \right)_{human} \times 100\%, \quad (1)$$

where A and m represent activities and organ masses, and the subscripts b and TB refer to the plasma and total body. Human organ masses from the Reference Man (8) were used. The cumulated radioactivities for C-11 DMO in man were then determined by a simple numerical integration of the data for percent injected dose per organ (the area was assumed equal to the product of the average value and the time period, with the decay of C-11 taken into account).

Radiation absorbed doses were estimated using standard MIRD absorbed fraction techniques and data (9-12). Each estimate included contributions from the organ itself, all other individually identified organs, and the remainder of the body, with the "S" factor (radiation absorbed dose per unit cumulated radioactivity) for the remainder of the body computed as recommended by Coffey et al. (13). For organs not included in MIRD Pamphlet No. 11 (11), absorbed fraction data (14,15) were used with radionuclide decay schemes and nuclear parameters (16) and reciprocity (9).

Error analysis. The tissue-plasma partition coefficient (tissue-to-plasma concentration ratio) may be related to tissue and plasma pH and the pK_a of DMO (6.13) by the following simple expression (17):

$$\frac{C_t}{C_b} = p = \frac{10^{pH_t - pK_a} + 1}{10^{pH_b - pK_a} + 1}, \quad (2)$$

where C represents DMO concentration, p is the tissue-to-plasma partition coefficient, and the subscripts t and b refer to tissue water and plasma water. Tissue pH as defined by this equation is a weighted value representing the combined intracellular, extracellular, and vascular subcompartments. It has been assumed that C_t and C_p are equilibrium values and that pK_a is the same in plasma and tissue.

To investigate the feasibility of using PET protocols to estimate tissue pH from measurements of p , an error analysis of the above model was performed. Using standard error propagation formulae (18) and assuming $pK_a = 6.13$ and $pH_b = 7.4$, the standard deviation in measured tissue pH (σ_{pH}) was found to be related to the fractional standard deviation of the partition coefficient, σ_p/p , by:

$$\sigma_{pH} = \frac{8.52 p}{19.6p - 1} (\sigma_p/p) \quad (3)$$

The errors resulting from failure to reach equilibrium

have not been considered here but will be discussed later. The empirical formula of Budinger et al. (19) for the root mean-square-deviation (RMSD) of measured tissue radioactivity concentrations in PET regions of interest (ROIs), multiplied by two to account for randoms and attenuation noise, was used to estimate the errors in PET measurements. For a slice 20 cm in diameter from a 1400-cm³ brain (8), with an average brain-to-plasma partition coefficient for DMO of 0.4 (based on rat biodistribution data) and a PET camera sensitivity of 30,000 cps/ μ Ci/cc, the RMSD in a 1.5 \times 1.5 cm² ROI (1 cm nominal slice thickness) was estimated as:

$$RMSD = \frac{0.278}{p^{3/4} A_0^{1/2} I_f^{1/2}}, \quad (4)$$

where p represents the DMO tissue-to-plasma partition coefficient in the ROI, A_0 is the injected radioactivity in mCi, and I_f is a factor related to the effective imaging time in min for a radiopharmaceutical that decays during the imaging period. For a bolus injection this is given by:

$$I_f = e^{-\lambda t_0} (1 - e^{-\lambda t_f}) / \lambda, \quad (5)$$

where t_0 is the starting time (min) relative to the injection, t_f is the frame time (min), and λ is the physical decay constant for C-11 (0.034/min).

If errors in PET camera calibration and measured plasma radioactivity concentration are neglected, then the RMSD is a good approximation of σ_p/p , since p is a linear function of the brain radioactivity concentration, and may be used with Eq. (2) to estimate the standard deviation in measured tissue pH.

The above error analysis is directly applicable to measurements of brain pH. To investigate the errors involved in pH measurements in other organs (e.g., the heart), the expression for RMSD (Eq. 4) should be modified to account for the average uptake in the organ of interest and in the slice containing the organ.

RESULTS

Biodistribution and in vivo kinetics. The biodistribution of C-14 DMO in rats, expressed as organ-to-plasma DMO partition coefficients as a function of time after injection, is summarized in Table 1A. Table 1B includes values of the percent injected dose per organ as estimated for humans from the rat data. Equilibration is rapid (<5 min) for most vascular organs such as thyroid, heart, and liver, but requires 30-60 min for brain. Table 2 summarizes the effective "tissue pH" for each organ, determined using Eq. (1) and the 120-min biodistribution data from Table 1. These tissue pH values agree, to within 0.03-0.23 pH units, with the values of intracellular pH determined previously for rat liver, heart, and skeletal muscle (21,22).

The urine-to-plasma concentration ratio generally

TABLE 1A. BIODISTRIBUTION OF C-14 DMO IN VARIOUS RAT ORGANS, EXPRESSED AS TISSUE-PLASMA PARTITION COEFFICIENTS AS A FUNCTION OF TIME

Organ	Time (min)				
	5.0	15.0	30.0	60.0	120.0
Adrenals	0.488	0.443	0.485	0.437	0.447
Bladder wall	0.500	0.742	0.668	0.703	0.955
Bone, cortical	0.182	0.176	0.182	0.146	0.180
Bone, trabecular	0.240	0.248	0.229	0.269	0.252
Brain	0.168	0.294	0.376	0.422	0.405
Fat	0.099	0.194	0.142	0.093	0.150
Stomach wall	0.417	0.369	0.417	0.434	0.457
contents	0.072	0.061	0.074	0.137	0.012
Sml. intestine wall	0.496	0.471	0.443	0.588	0.546
contents	0.482	0.330	0.593	0.569	0.618
Upper lg. intes. wall	0.310	0.470	0.603	0.986	0.649
contents	0.120	0.301	0.698	0.864	1.004
Lower lg. intes. wall	0.435	0.523	0.565	0.569	0.617
contents	0.369	0.343	0.501	0.963	0.550
Heart	0.476	0.476	0.490	0.462	0.511
Kidneys	0.441	0.452	0.456	0.405	0.455
Liver	0.520	0.504	0.490	0.516	0.528
Lungs	0.514	0.572	0.654	0.558	0.562
Muscle	0.375	0.446	0.421	0.382	0.396
Ovaries	0.503	0.507	0.494	0.543	0.544
Pancreas	0.388	0.395	0.408	0.382	0.397
Skin	0.359	0.457	0.508	0.482	0.534
Spleen	0.411	0.420	0.420	0.408	0.441
Testes	0.113	0.198	0.328	0.392	0.394
Thyroid	0.431	0.435	0.432	0.421	0.446
Uterus	0.577	0.593	0.528	0.612	0.655
Blood*	3.99	3.30	3.15	2.95	2.84

* Plasma concentration/whole-body concentration.

followed urine pH, with alkaline urine containing relatively large amounts of DMO and acidic urine having a lower DMO concentration. In acidic urine the radioactivity concentration remained less than half that of plasma.

Estimates of absorbed radiation dose. For the organs studied, estimates of cumulated radioactivity and radiation absorbed dose per administered mCi are summarized in Table 3. (Urine cumulated radioactivity was estimated assuming a urine-to-plasma concentration ratio of 2.) The listed cumulated radioactivities for individual organs, excluding blood and urine, accounted for 96% of the total administered radioactivity. Urine accounted for 0.5% of the total administered radioactivity, whereas blood corresponded to approximately 20%. The sum of the individual cumulated radioactivities listed in Table 3 is thus 16% greater than the actual total.

This undoubtedly results from the presence of blood in several organ samples, especially muscle. Only blood in the heart chambers (500 g) was considered for the absorbed dose estimates. Estimates of radiation absorbed dose ranged from 8–23 mrad/mCi, with the maximum dose to small intestine, uterus, and heart.

Feasibility of C-11 DMO PET studies. Small differences in the tissue-blood partition coefficient for DMO correspond to large differences in calculated tissue pH for pH <7.0, hence a larger uncertainty should be present in C-11 DMO PET measurements of *r*pH that fall within this range. This is clearly illustrated in Fig. 1, in which the standard deviation in measured tissue pH (expressed in pH units) is plotted as a function of the relative standard deviation in the partition coefficient at several values of tissue pH. The uncertainty in pH measurements is more sensitive to the uncertainty in

TABLE 1B. BIODISTRIBUTION OF C-14 DMO, EXPRESSED AS PERCENT INJECTED DOSE PER ORGAN (%ID/O) IN MAN AS A FUNCTION OF TIME

Organ	Time (min)				
	5.0	15.0	30.0	60.0	120.0
Adrenals	0.0389	0.0292	0.0306	0.0258	0.0254
Bladder wall	0.128	0.157	0.135	0.133	0.174
Bone, cortical	4.15	3.32	3.28	2.46	2.92
Bone, trabecular	1.37	1.17	1.03	1.13	1.02
Brain	1.34	1.94	2.37	2.49	2.30
Fat	7.05	11.4	7.99	4.90	7.61
Stomach wall	0.357	0.261	0.281	0.274	0.278
contents	0.103	0.0719	0.0833	0.144	0.122
Sml. intestine wall	1.81	1.42	1.28	1.59	1.42
contents	1.10	0.622	1.07	0.959	1.00
Upper lg. intes. wall	0.369	0.463	0.567	0.868	0.550
contents	0.150	0.312	0.691	0.801	0.896
Lower lg. intes. wall	0.397	0.394	0.407	0.384	0.401
contents	0.284	0.218	0.304	0.548	0.301
Heart	0.895	0.741	0.728	0.643	0.684
Kidneys	0.779	0.661	0.636	0.529	0.572
Liver	5.34	4.28	3.97	3.91	3.86
Lungs	2.93	2.70	2.94	2.35	2.28
Muscle	59.9	58.9	53.0	45.1	45.0
Ovaries	0.0315	0.0263	0.0245	0.0252	0.0243
Pancreas	0.221	0.186	0.184	0.161	0.161
Skin	5.32	5.60	5.94	5.28	5.63
Spleen	0.422	0.356	0.340	0.309	0.322
Testes	0.0225	0.0327	0.0517	0.0578	0.0559
Thyroid	0.0491	0.0410	0.0389	0.0355	0.0362
Uterus	0.263	0.224	0.190	0.206	0.213

TABLE 2. EFFECTIVE RAT-TISSUE pH DETERMINED FROM BIODISTRIBUTION DATA

Organ	Tissue pH*	Literature values of intracellular pH
Brain	7.04	
Stomach wall	7.11	
Sml. intestine wall	7.19	
Upper lg. intes. wall	7.26	
Lower lg. intes. wall	7.27	
Heart	7.18	7.04 (21), 6.95 (22)
Kidneys	7.13	
Liver	7.22	7.23 (21), 7.11 (22)
Lungs	7.20	
Muscle	7.06	6.93 (21), 6.85-6.95 (22)
Ovaries	7.22	
Spleen	7.10	
Testes	7.05	

* Based on Eq. (2) and 120-min biodistribution data from Table 1.

partition coefficient at low tissue pH than at high tissue pH.

In Fig. 2 the predicted standard deviation of measured tissue pH (resulting from counting statistics) in a homogeneous 1.5- by 1.5-cm² ROI is plotted as a function of pH for a 20-mCi administered dose when equilibration periods of 15, 30, and 45 min, elapse before a 15-min PET data collection period. As is apparent from the figure, counting statistics should permit the determination of regional pH to within 0.10 pH unit for pH >6.5, which is well below the pH of normal brain tissue. However, tissue pH <6.25 cannot be determined to this accuracy unless larger doses of C-11 DMO are administered and shorter equilibration times are possible.

DISCUSSION

The biodistribution data for C-14 DMO in rats reveals a rapid equilibration in most tissues (<5 min for most vascular organs) and approximately 30-60 min for brain. Values of tissue pH for rat tissue, heart and skeletal

TABLE 3. CUMULATED RADIOACTIVITIES AND ESTIMATED RADIATION ABSORBED DOSES FOR C-11 DMO

Organ	Cumulated radioactivity $\mu\text{Ci-h/mCi}^*$	Self-dose [†] mrad/mCi [*]	Total dose [‡] mrad/mCi [*]
Adrenals	0.16	10	17
Bladder wall	0.73	8.4	14
Bladder contents [§]	2.3	—	—
Blood	97	—	—
Bone, cortical	18	3.4	8.3
Bone, trabecular	6.2	0.80	9.2
Brain	10	8.8	11
Fat	42	1.7	15
Stomach wall	1.6	4.3	10
contents	0.50	—	—
Sml. intestine wall	8.0	17	23
contents	5.0	—	—
Upper lg. intest. wall	2.8	12	19
contents	2.5	—	—
Lower lg. intest. wall	2.1	13	19
contents	1.7	—	—
Heart wall	4.0	15	21
Kidneys	3.5	11	17
Liver	23	15	19
Lungs	14	14	19
Muscle	285	12	15
Ovaries	0.14	12	19
Pancreas	0.99	9.9	17
Skin	29	9.9	13
Spleen	1.9	11	16
Testes	0.21	5.7	10
Thyroid	0.22	10	14
Uterus	1.2	12	23
Total body	491	11	11

[†] Due to radioactivity in organ itself.

[‡] Due to radioactivity in organ, other individually identified organs, and the remainder of the body.

* Administered mCi.

[§] Based on urine-to-plasma concentration ratio of 2.

muscle estimated using these data were found to be in good agreement with other values reported in the literature.

C-11 DMO may be produced in sufficient quantities (>20 mCi) to permit quantitation of regional brain tissue pH using PET, for tissue pH >6.5. For such studies the various organs of the body would receive radiation absorbed doses ranging from 170–460 mrad/20 mCi. Maximum doses of 420–460 mrad/20 mCi would be received by the uterus, small intestine, and heart walls.

The error introduced by the assumption of brain-plasma equilibration was not considered in Fig. 2. Equilibration of C-14 DMO in rat brain was found to require 30–60 min (the brain-plasma partition coefficient increased 10% from 30 to 60 min, and no measurable increase was noted thereafter). Imaging at 60 min may result in suboptimal imaging statistics due to decay of C-11 ($T_{1/2} = 20.4$ min). The rat data suggest that images at 30 min could contain an error of approximately 0.05 pH (for $6.5 < \text{pH} < 7.0$) resulting from the incorrect assumption of brain-plasma equilibration.

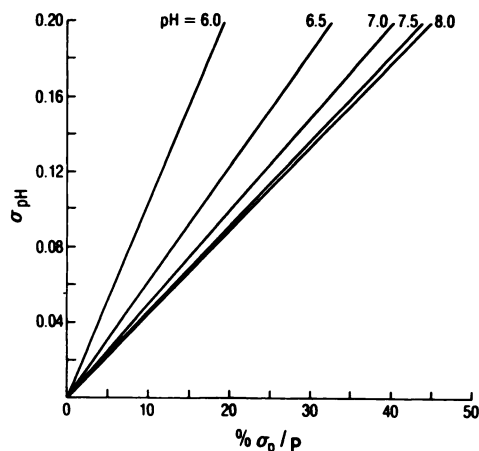


FIG. 1. Standard deviation in measured tissue pH, σ_{pH} , (in pH units) as function of fractional standard deviation in tissue partition coefficient, σ_p/p , for various values of tissue pH.

Alternatively, by exploiting the dynamic capabilities of new, sensitive multi-slice PET instruments, kinetic data could be used to extrapolate the asymptotic value of the brain-blood partition coefficient. DMO equilibration in poorly perfused brain may be slower than in normal brain, limiting the accuracy of tissue pH measurements with DMO in cerebrovascular disease.

At extremely low tissue pH, both (a) poor imaging statistics and (b) brain-tissue blood content limit the accuracy of derived tissue pH measurements. Since the equilibrium tissue concentration of DMO is low at acidic pH, brain tissue pH <6.5 cannot be determined accurately unless larger doses of C-11 DMO are administered or shorter equilibration times are possible. At a normal brain tissue pH of about 7.0, error introduced by neglecting a 3% cerebral blood volume can be shown to be only 0.014 pH units, but this error approaches 0.10 pH unit at a pH of 6.5.

Tissue pH, as measured with DMO, is an aggregate pH reflecting the pH of intracellular and extracellular

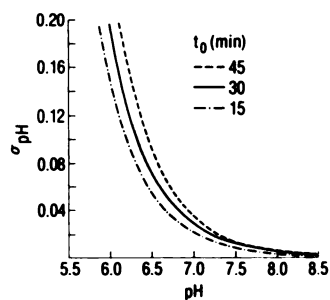


FIG. 2. Error in measured regional brain tissue pH due to counting statistics (σ_{pH} in pH units), as function of tissue pH, for 15-min PET imaging period (PET sensitivity 30,000 cps/ μ Cl/cc) begun at times $t_0 = 15, 30,$ and 45 min after injection of 20 mCi C-11 DMO. These estimates assume overall brain-to-plasma partition coefficient of 0.4, and do not take into account error introduced by incomplete brain-blood equilibration.

compartments. Estimation of intracellular pH requires knowledge of extracellular fluid pH as well as of the relative size of these compartments (5,23). Nevertheless, tissue pH may be considered as a potentially useful index of tissue acid-base status. PET techniques using C-11 DMO to measure tissue pH should provide important new information about cerebral acid-base status and metabolism in health and disease.

ACKNOWLEDGMENTS

The authors are grateful to Ms. Cathy Davis (New York University, New York, NY) for technical assistance with the biodistribution studies and to Ms. Adele Ahronheim for preparing the manuscript.

This work was supported in part by Award No. 15665 from the National Institutes of Health.

REFERENCES

1. RAICHLER ME, GRUBB RL, HIGGINS CS: Measurement of brain tissue carbon dioxide content in vivo by emission tomography. *Brain Res* 166:413-417, 1979
2. LOCKWOOD AH, FINN RD: 11 C-Carbon dioxide fixation and equilibration in rat brain: effects on acid-base measurements. *Neurology* 32:451-454, 1982
3. BORON WF, ROOS A: Comparison of microelectrode, DMO, and methylamine methods for measuring intracellular pH. *Am J Physiol* 231:799-809, 1976
4. HINKE JA, MENARD MR: Evaluation of the DMO method for measuring intracellular pH. *Respir Physiol* 33:31-40, 1978
5. PELLIGRINO DA, MUSCH TI, DEMPSEY JA: Interregional differences in brain intracellular pH and water compartmentation during acute normoxic and hypoxic hypocapnea in the anesthetized dog. *Brain Res* 214:387-404, 1981
6. GINOS JZ, TILBURY RS, HABER MT, et al: Synthesis of [11 C]5,5-dimethyl-2,4-oxazolidinedione for studies with positron tomography. *J Nucl Med* 23:255-258, 1982
7. ROLLINS DE, REED DJ: Transport of DMO out of cerebrospinal fluid of rats. *Am J Physiol* 219:1200-1204, 1970
8. SNYDER WS, COOK MJ, NASSET ES, et al: *Report of the Task Group on Reference Man*, ICRP Publication 23, New York, Pergamon Press, 1974
9. LOEVINGER R, BERMAN M: A schema for absorbed dose calculations for biologically distributed radionuclides. MIRD Pamphlet No. 1, *J Nucl Med*: Suppl No. 1, 7-14, 1968 (revised 1976)
10. CLOUTIER RJ, WATSON EE, ROHRER RH, et al: Calculating the radiation dose to an organ. *J Nucl Med* 14:53-55, 1973
11. SNYDER WS, FORD MR, WARNER GG, et al: "S" absorbed dose per unit cumulated activity for selected radionuclides and organs, MIRD Pamphlet No. 11. New York, Society of Nuclear Medicine, 1975
12. SNYDER WS, FORD MR, WARNER GG, et al: *A tabulation of dose equivalents per microcurie-day for source and target organs of an adult for various radionuclides*. Oak Ridge National Laboratory Report ORNL-5000, 1974, pp 16-19
13. COFFEY JL, WATSON EE: Calculating dose from remaining body activity: a comparison of two methods. *Med Phys* 6(4):307-308, 1979
14. SNYDER WS, FORD MR, WARNER GG, et al: Estimates of absorbed fractions for monenergetic photon sources uniformly

- distributed in various organs of a heterogeneous phantom. MIRD Pamphlet No. 5, *J Nucl Med*: Suppl No. 3, 1969 (revised 1978), pp 16-17
15. COFFEY JL, CRISTY M, WARNER GG: Specified absorbed fractions for photon sources uniformly distributed in heart chambers and heart wall of a heterogeneous phantom. *J Nucl Med* 22(1):65-71, 1981
 16. DILLMAN LT, VON DER LAGE FL: *Radionuclide decay schemes and nuclear parameters for use in radiation-dose estimation*, MIRD Pamphlet No. 10. New York, Society of Nuclear Medicine, 1975
 17. JUNCK L, BLASBERG R, ROTTENBERG DA: Brain and tumor pH in experimental leptomeningeal carcinomatosis. *Trans Am Neurol Assoc* 106: 298-301, 1981.
 18. YOUNG HD: *Statistical Treatment of Experimental Data*, New York, McGraw-Hill Book Company, Inc., 1962, pp 96-101
 19. BUDINGER TF, DERENZO SE, GREENBERG WL, et al: Quantitative potentials of dynamic emission computed tomography. *J Nucl Med* 19:309-315, 1978
 20. ALTMON PL, DITTMER DS: *Biology Data Book; Volume I*. Bethesda, Maryland, Federation of American Societies for Experimental Biology, pp 395-396, 1972
 21. WALKER WD, GOODWIN FJ, COHEN RD: Mean intracellular hydrogen ion activity in the whole body, liver, heart and skeletal muscle of the rat. *Clin Sci* 36:409-417, 1969
 22. CALDERWOOD SK, DICKSON JA: Rapid method for measuring intracellular pH in vivo. *Cell Biol Int Rep* 2:327-337, 1978
 23. LEVIN VA, FENSTERMACHER JD, PATLAK CS: Sucrose and inulin space measurements of cerebral cortex in four mammalian species. *Am J Physiol* 219:1528-1533, 1970

SNM Conjoint Congress

February 1-6, 1984

Sheraton World Hotel

Orlando, Florida

In cooperation with the Computer and Instrumentation Councils and Technologist Section, the Society of Nuclear Medicine invites physicians, basic scientists, and technologists to attend the 3rd Conjoint Congress. Join us February 1-6, 1984 in Orlando, Florida to examine one of the most challenging developments in nuclear medicine: **The Technology of NMR**. Examine NMR instrumentation, imaging techniques for spacial encoding, problems of pulse sequencing, image processing and display, spectroscopy, and system evaluation.

In addition to the Councils' Program, technologists will present concurrent sessions that examine NMR, SPECT, monoclonal antibodies, and more. Section and Council members can expect their programs in November and December, respectively. For more information write: SNM Meetings Department, 475 Park Avenue South, New York, NY 10016, or call (212)889-0717.

Schedule

Wednesday, February 1	8:00 a.m.-10:00 p.m.	Technologist Section Committee Meetings
Thursday, February 2	8:00 a.m.- 5:00 p.m.	Technologist Section National Council Meeting
Friday, February 3	8:00 a.m.-10:00 p.m.	SNM Committee Meetings
	1:00 p.m.- 5:00 p.m.	Technologist Section Educational Program
Saturday, February 4	8:30 a.m.- 5:00 p.m.	SNM Board of Trustees Meeting
	8:30 a.m.- 5:00 p.m.	Technologist Section Educational Program
Sunday, February 5	8:30 a.m.- 5:00 p.m.	Computer & Instrumentation Councils' Symposia on NMR
	8:30 a.m.-12:00 p.m.	Technologist Section Educational Program
Monday, February 6	8:30 a.m.- 5:00 p.m.	Computer & Instrumentation Councils' Symposia on NMR